Fermilab

Doc Number: BooNE-TN-076
Version: 1.0

Some Preliminary Considerations on Scattered Light Response in MiniBooNE

Bruce C. Brown
Beams Division, Main Injector Department
Fermi National Accelerator Laboratory *
P.O. Box 500
Batavia, Illinois 60510

19-June-2003

Contents

*Operated by the Universities Research Association under contract with the U. S. Department of Energy

Abstract

Introducing scattered light as a significant signal component in the response of the MiniBooNE detector suggests (requires) new fitting models. Late light due to scattering of the Cherenkov light provides a space-time response correlated with the amplitude and direction of the Cherenkov light source region which should be employed to distinguish it from scintillation. A scattering sensitivity function is described which expresses the scattered light amplitude as a function of the extra delay due to path length. Responses averaged over the tank impose constraints on the relations between late light fraction, scattering length and scintillation fraction which can be employed to understand the scattering model.

1 Introduction

The initial fitting models for light produced in the MiniBooNE detector have assumed Cherenkov light (prompt and directional) plus scintillation light (exponentially decaying and isotropic). Recent work on the observed time distribution combined with measurements of the scintillation yield of the oil appear to demand significant scattering. Since we wish to employ scintillation signals to separate physics processes, we need to seek ways to avoid contaminating late light scintillation signals with scattering. We note that the path of the Cherenkov light is well determined by the fitting processes so scattering from that path occurs at predictable times over a limited region in space. The response from that scattering, as observed by any phototube, has a well determined sensitivity function whose time axis is imposed by the added path lengths. For isotropic scattering, the amplitude of the sensitivity function reflects the solid angle subtended by the phototube from the scattering location. If the scattering is not isotropic, the amplitude function will be accordingly modified. Since the frame for expressing this sensitivity function is anchored on the Cherenkov production point, angular effects in the scattering, if present, can be accommodated.

This analysis is motivated by the three observations

1. Ryan Patterson and his colleagues observe that the late light photons from the calibration lasers are more than a third as numerous as the prompt photons. [Reported at several recent MiniBooNE meetings].

2. Hans-Otto Meyers described the scattering from a laser beam in a small flask of oil. This was a visual inspection which suggested that

the scattering may be isotropic [February 27-28, 2003 Big MiniBooNE Mtg].

3. Reports from the scintillation measurements at IUCF which report a scintillation fraction of 5.7%, much less than the 25% which was a previously discussed number.

Together, these suggest that important new considerations are required to optimize event fitting for scintillation sensitivity.

This preliminary introduction will attempt to provide some sense of the magnitude of these effects, describe an analytic approach to adding them to the fitting procedure and explore constraints on the magnitude of scattered light and scattering lengths based on properties of event averages.

2 Sensitivity Function Geometry

The largest differences in scattering sensitivity occur as a function of the path length of the Cherenkov light, which in turn is much different for inward *vs.* outward pointing tracks. With this in mind, it seems natural to consider a geometry with the primary axis pointed in the direction of the particle which is emitting the light. Let this become the z direction and let the z axis go through the middle of the tank (just about the usual tank frame for the most frequently produced muons). If the track axis does not pass through the tank center, we will define its offset as being in the x direction. The particle track will be fully described in this plane although the Cherenkov and scattered light will, of course require the y dimension. An illustration of the geometry to consider is shown in Figure 1.

Light in oil travels at $v = c/n_{group}$. Let us call the radius of the optical barrier R and define the phototube positions with the vector $\vec{R}$ (from the center of the tank). We describe the source position for the Cherenkov light as the point $(\vec{P} = x, y = 0, z)$ with $+z$ in the direction of particle travel and origin at the tank center. The cone of Cherenkov light will be emitted at the Cherenkov angle θ_c where $\cos\theta_c = 1/n_{phase}$. Let $\vec{S}(t)$ trace out the path of the Cherenkov light with origin at the light production point. In this manner we find that the light scattered at a given point along the path $\vec{S}(t)$ will happen at tank location $\vec{P}+\vec{S}(t)$. The vector to the detecting phototube is $\vec{P}+\vec{S}(t)-\vec{R}$. The time of arrival at the phototube is $t_R = t+\frac{1}{v}|\vec{P}+\vec{S}(t)-\vec{R}|$. Assuming we choose to correct all observed times as if the light was produced where the Cherenkov light was produced, the correction is $t_{corr} = \frac{1}{v}|\vec{P}-\vec{R}|$.

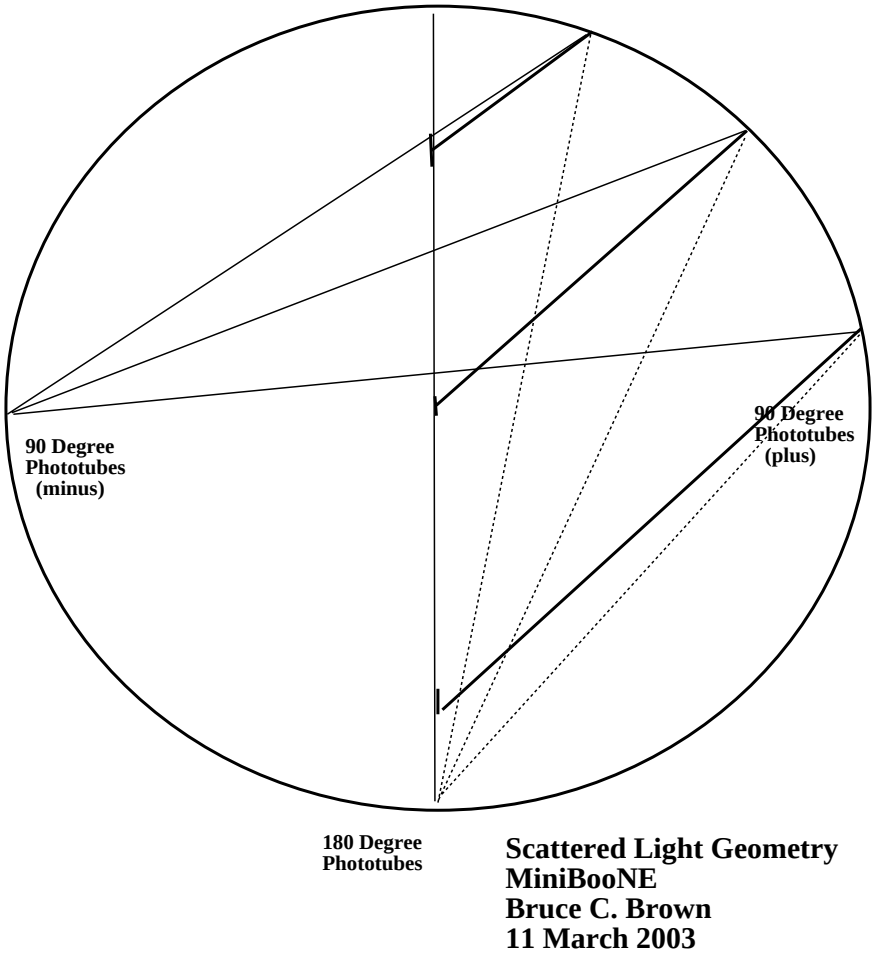

Figure 1: Geometry for Cherenkov Light Scattering in MiniBoone.

We will use $t_{Rc} = t_R - t_{corr}$ as the independent variable for the sensitivity function.

For isotropic scattering, the amplitude of the sensitivity function is obtained simply by the solid angle presented by the detector. A proper calculation will employ the phototube geometry. For illustration purposes, we will simply note that the solid angle is proportional to the distance from scattering point to phototube which is $|\vec{P} + \vec{S}(t) - \vec{R}|$. Adding the proper phototube solid angle is straightforward as is multiplying by a form factor to account for angular dependence of the scattering.

3 Sensitivity Function Calculation in 2-D

Let us define a scattering sensitivity function $T(\vec{P}, \vec{R}, t_{Rc})$ as the ratio of the scattered Cherenkov light produced at $\vec{P}$ which is detected at position $\vec{R}$ at time t_{Rc}. This is obtained by integrating the scattered light fraction at each $\vec{S}(t)$ from $t = 0$ to the point where the Cherenkov light strikes the optical barrier which occurs when $|\vec{P} + \vec{S}(t)| = R$. A full calculation requires consideration of $\vec{S}$ in all directions along the cone. This integration is easy to describe but considering only the two dimensional case is even easier. A spreadsheet can be quickly constructed to calculate the time delay and solid angle for each point along the Cherenkov light path. Assuming that the scattering length is long compared to the path length, the scattered light intensity will be nearly independent of the scattering point. We will next present a calculation in this approximation.

The path length for Cherenkov light varies greatly over the fiducial area of the detector. For a particle traveling on axis, rays all around the cone have the same length to the optical barrier. Figure 2 shows this path length *vs.* light source position along z. If we consider $z = \pm 4.5$ m the Cherenkov travel time (path length) varies from 7 to 37 ns. Thus the scattered light background varies $\times 5$ over the fiducial volume (One might guess that the ratio for off axis particles falls between these limits).

The spreadsheet calculation has been set up to provide the sensitivity function with time and solid angle as adjacent column pairs Calculations are carried out for phototube angles of $-180^o, \pm 135^o, \pm 90^o, \pm 45^o$ and 0^o. Worksheets for 7 z positions have been cloned from the initial worksheet. The graphical presentation has been accomplished for two selected angles by transferring the results to files for use in the xmgr plotting package. Figure 3 shows a case where the 2-D calculation is complete. Light detected at -180^o $(z = -R)$ has the same geometry for any angle in the Cherenkov cone so this figure shows the scattered light variation for the various production points along the axis. The vertical axis is not properly normalized but is simply $1/m^2$. The curve for -4.5 m rises to 1 at its peak. In contrast, the peak for the center of the tank is 0.03 $1/m^2$ and for the far end of the tank only 0.01 $1/m^2$ No first scatter Cherenkov light from 4.5 m arrives with greater than a 12 ns added delay. Even from z=0, the maximum delay is 27 ns. If sufficient scintillation light is detected in this angular range, the scattering can be removed with a time cut.

Light detected by the phototubes at 90^o have very different responses from the various parts of the cone, even from the same light production

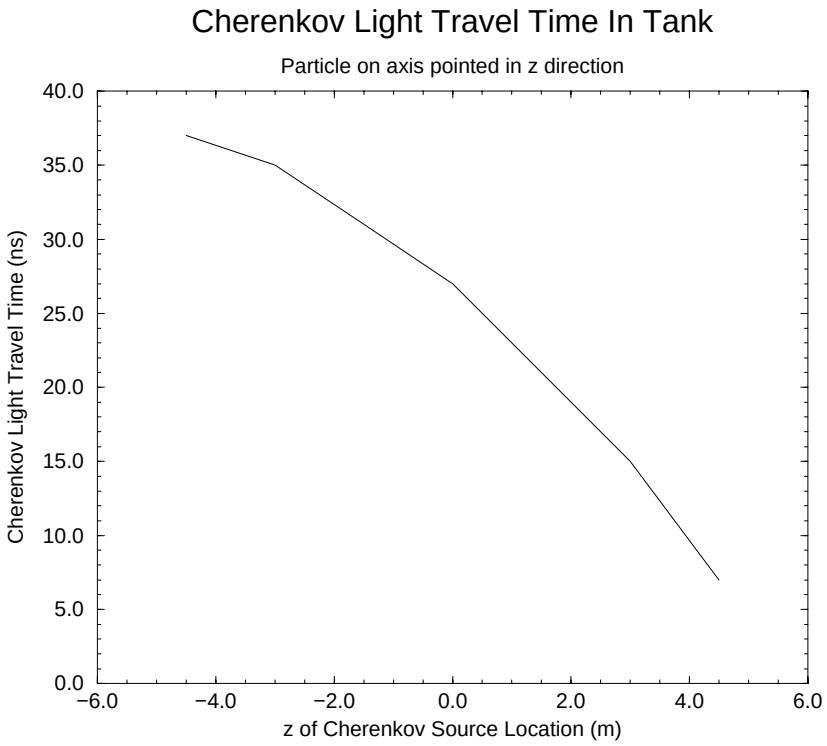

Figure 2: Path length (in ns) of Cherenkov light produced on axis as a function of production location.

point. Figure 4 show the 2-D calculation with light from a ray in the $+x$ direction. We label the detector at $(x = R, z = 0)$ as $+90^o$ while the one at $(x = -R, z = 0)$ as -90^o. Especially for the Cherenkov light produced near z =-4.5 m, the sensitivity for this ray gets to be very large because the scattering occurs very near to the phototube. However, non-trivial delays are still apparent. Delays from 2 to nearly 6 ns occur for the region where the solid angle is large. Although the solid angle drops for the light produced for $z > -3$ m, the time delays get larger. To display the range of sensitivity for both toward $(+90^o)$ and away $-90^o)$ tubes, we show the data with three vertical scales. One would expect the sensitivity determined by a 3-D calculation to find that the delay and solid angle for the rays other than those in the x plane would have intermediate values.

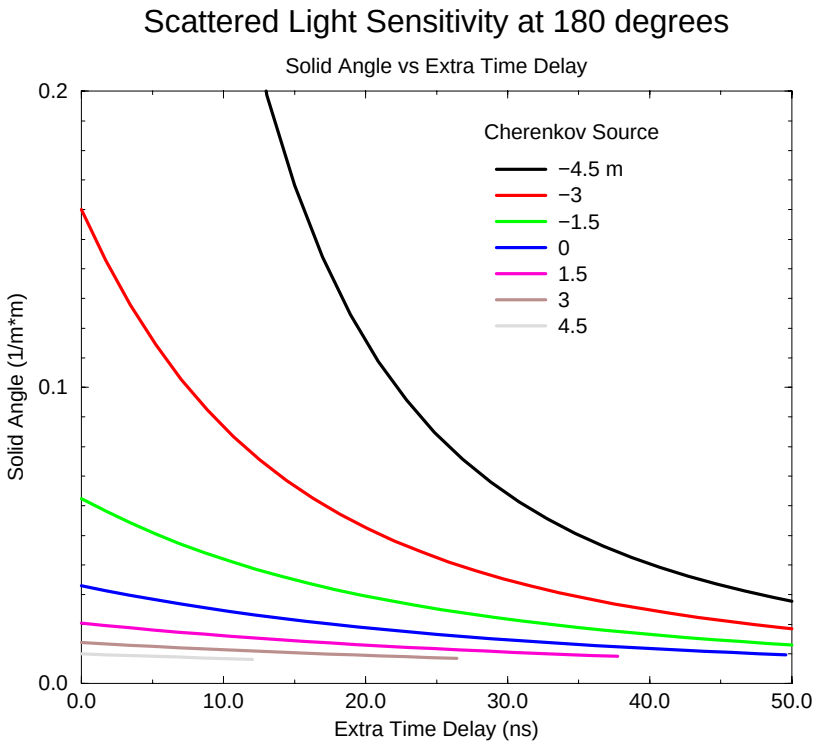

Figure 3: Sensitivity function for phototube at 180^o or $z = -R$.

The graphs shown for the sensitivity function shows the sensitivity (solid angle) for a series of points along the Cherenkov cone spaced at 1 ns intervals. To obtain a sensitivity suitable for fitting, one is required to do the proper integral so that the sensitivity per unit delayed time is made available. The sensitivity calculation will also be modified when the attenuation of the Cherenkov light due to scattering (and perhaps absorption) reduces the light available for scattering as the path length grows. This modification will be up to perhaps $20 - 30\%$ for the longest path lengths. One also notes that the longest delayed scattering paths involve light which travels more than 70 ns extra and will thereby have a non-trivial re-scattering probability.

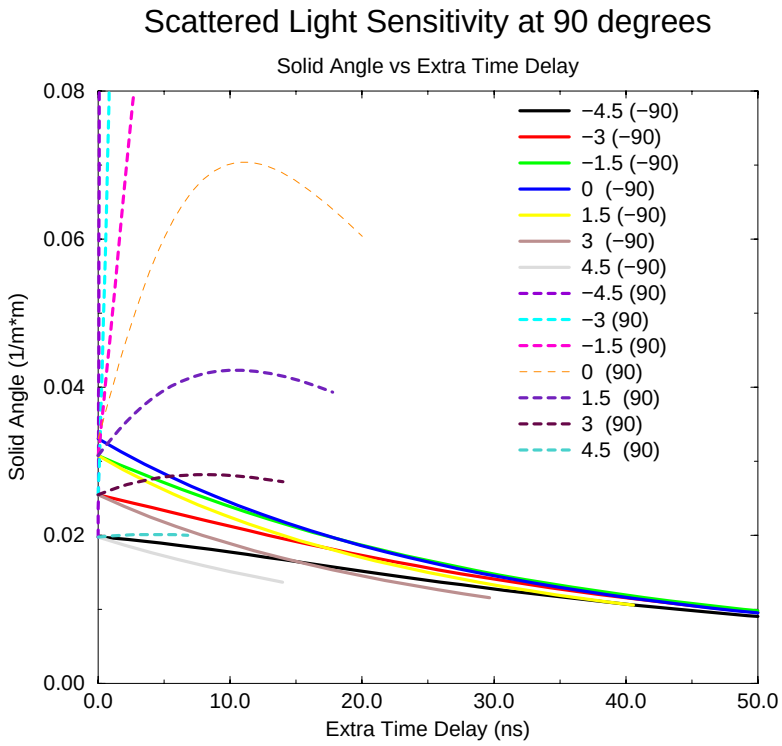

Figure 4: Sensitivity function for phototube at $\pm 90^o$ Scaled for sensitivity at -90°.

4 Constraints on Scattering from Average Event Properties

Using measurements of event properties averaged over the detector volume, properties of laser calibration events and measured scintillation yield, we can constrain properties of the scattering and absorption of light in our oil. Let us describe the light emission and transmission properties to obtain relations between them using the separation into prompt and delayed light. We will take averages over the spectrum as well. We obtain a source location for muon or electron events from the reconstructed Cherenkov cone. Using this source location we correct the observed time for the delay along the assumed path. Let us define C_{h0} as the emitted Cherenkov light. $C_h(s)$ is

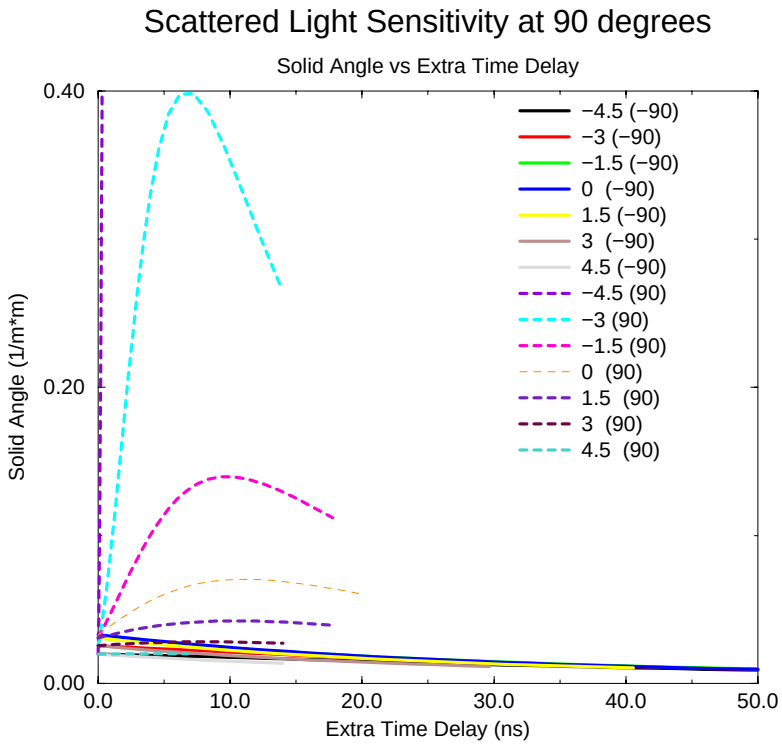

Figure 5: Sensitivity function for phototube at $\pm 90^o$. Scaled for sensitivity at $+90^o$.

the Cherenkov light remaining at position s where $s = |\vec{S}(t)|$.

$$C_h(s) = C_{h0} e^{-s/L_S} e^{-s/L_A} \sim C_{h0}[1 - \frac{s}{L_S}][1 - \frac{s}{L_A}] \qquad (1)$$

where L_S is the scattering length and L_A is the absorption length.[1] Light in the cone will come at time zero after correction for its path in oil. Its magnitude will be

[1] The attenuation measured in the oil tests includes the absorption of light plus most (some) of the scattering which is isotropic (forward). The details will depend upon the angular dependence of the scattering and the angular acceptance of the attenuation measurement systems.

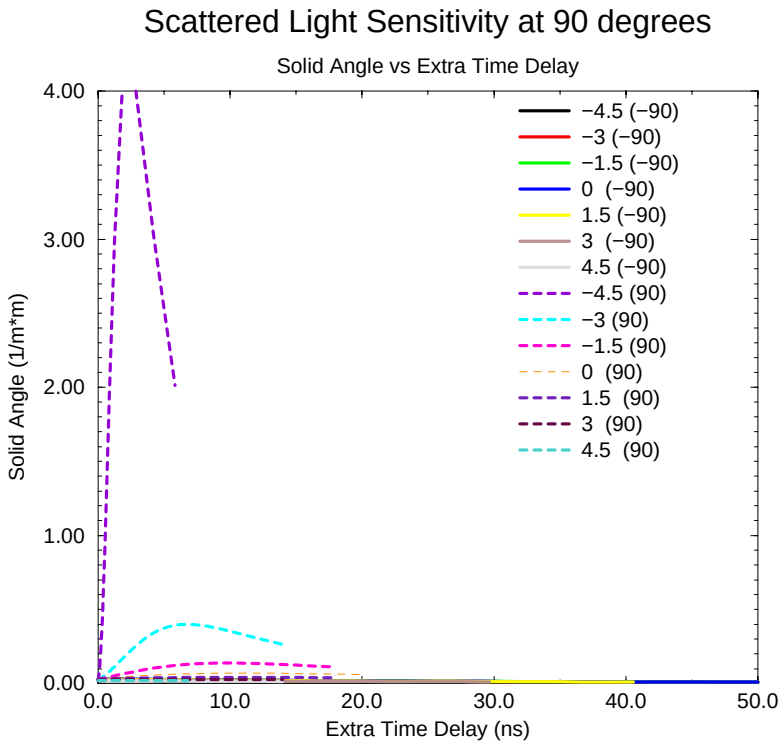

Figure 6: Sensitivity function for phototube at $\pm 90^o$. Scaled for sensitivity at $+90^o$ and entrance to tank.

$$C_h(< s >) \sim C_{h0}[1 - \frac{< s >}{L_S} - \frac{< s >}{L_A}]. \tag{2}$$

We can write similar equations for the scintillation and laser light

$$S_c(< s_S >) \sim S_{c0}[1 - \frac{< s_S >}{L_S} - \frac{< s_S >}{L_A}] \tag{3}$$

$$L_{aser}(< s_L >) \sim L_{aser0}[1 - \frac{< s_L >}{L_S} - \frac{< s_L >}{L_A}] \tag{4}$$

Assuming that the scattering and absorption lengths are long compared with the path lengths, we can get a first order estimate of the scattered light

fraction assuming that the light is not substantially attenuated. We find

$$C_{hS}(< s >) \sim C_{h0}\frac{< s >}{L_S}. \tag{5}$$

$$S_{cS}(< s_S >) \sim S_{c0}\frac{< s_S >}{L_S} \tag{6}$$

$$L_{aserS}(< s_L >) \sim L_{aser0}\frac{< s_L >}{L_S} \tag{7}$$

4.1 Constraint from Laser Light Time Distribution

Using this description, let us consider constraints from the laser calibration studies.

$$\frac{L_{aserS}(< s_L >)}{L_{aser}(< s_L >)} = [\frac{< s_L >}{L_S}]/[1 - \frac{< s_L >}{L_S} - \frac{< s_L >}{L_A}] \tag{8}$$

$$\frac{L_{aser}(< s_L >)}{L_{aserS}(< s_L >)} = [\frac{L_S}{< s_L >} - 1 - \frac{L_S}{L_A}] \tag{9}$$

$$\frac{L_S}{< s_L >} = \frac{L_{aser}(< s_L >)}{L_{aserS}(< s_L >)} + 1 + \frac{L_S}{L_A} \tag{10}$$

$$\frac{1}{L_A} = \frac{1}{< s_L >} - \frac{1}{L_S}[\frac{L_{aser}(< s_L >)}{L_{aserS}(< s_L >)} + 1] \tag{11}$$

From a histogram of the measured arrival time for laser events, one can fit the prompt peak and obtain its area (total photons)[2]. The total number of events in the histogram provides the sum of prompt and late light. For a central flask, Ryan Patterson has reported that prompt light is 74% of the total light detected. This implies $L_{aserS}(< s_L >)/L_{aser}(< s_L >)$ = .26/.74 =.35 and $L_{aser}(< s_L >)/L_{aserS}(< s_L >)$ =2.85. The mean path for the laser light is very near the radius of the light barrier (and phototubes) – 5.5 m. Figure 7 expresses this equation for various values of prompt/late light. The limit on the scattering length from this corresponds to the point where the inverse absorption length is zero. This occurs for an attenuation length which is the same as the scattering length, $L_S = s_L[1+\frac{L_{aser}(<s_L>)}{L_{aserS}(<s_L>)}]$= 21 m. Also consistent with this prompt/late ratio is an attenuation length of 10 m, absorption length of 15 m and a scattering length of 33 m.

[2]Thanks to Calibration Group for this result provided to me by Ryan Patterson

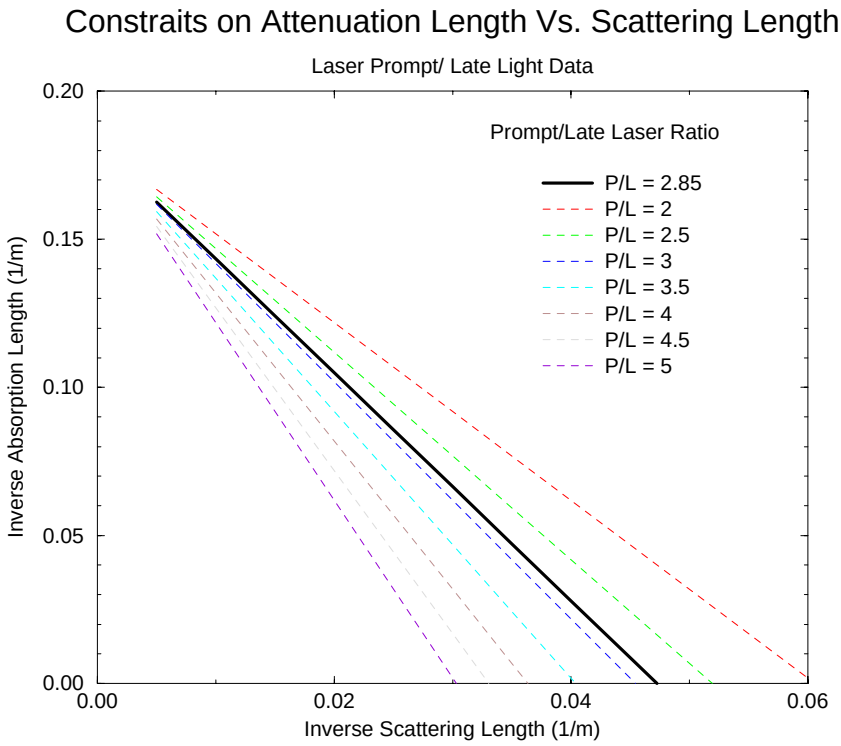

Figure 7: Based on the measured prompt/late light fraction (solid black line), the constraint between inverse absorption length and inverse scattering length is obtained. The sensitivity to late light is shown by the dashed curves corresponding to other values of prompt/late light.

4.2 Constraint from Time Distribution of Light from Michels

We can likewise obtain a constraint equation to describe light detected from the Michel Electrons. Again the analysis[3] employs the histogram of hit number *vs.* time. The time is corrected using the fit source location to determine a light path length but no attenuation correction is applied. The prompt/late light can be expressed as

[3]Let me thank Bonnie Flemming for describing this to me.

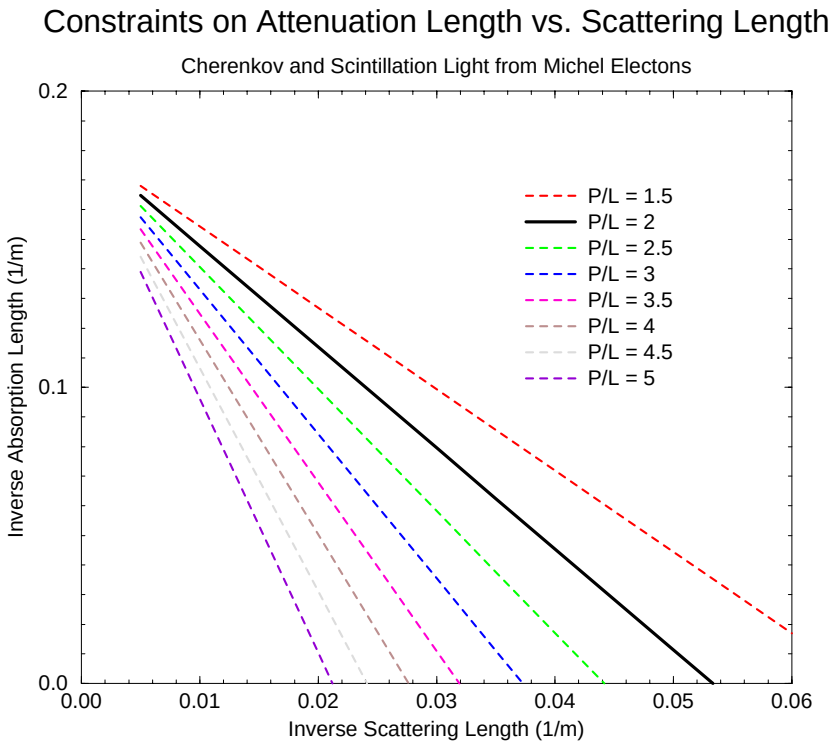

Figure 8: Based on the measured prompt/late light fraction (solid black line), the constraint between inverse absorption length and inverse scattering length is obtained. The sensitivity to late light is shown by the dashed curves corresponding to other values of prompt/late light. Scintillation/Cherenkov = 0.06 is assumed.

$$\frac{P_{rompt}}{L_{ate}} = \frac{C_h(< s >)}{C_{hS}(< s >) + S_c(< s >) + S_{cS}(< s >)} \tag{12}$$

$$\frac{P_{rompt}}{L_{ate}} = [1 - \frac{< s >}{L_S} - \frac{< s >}{L_A}]/[\frac{< s >}{L_S} + \frac{S_{c0}}{C_{h0}}[1 - \frac{< s >}{L_A}] \tag{13}$$

$$\frac{1}{L_S}\frac{P_{rompt}}{L_{ate}} + \frac{P_{rompt}}{L_{ate}}\frac{S_{c0}}{C_{h0}}[\frac{1}{< s >} - \frac{1}{L_A}] = [\frac{1}{< s >} - \frac{1}{L_S} - \frac{1}{L_A}] \tag{14}$$

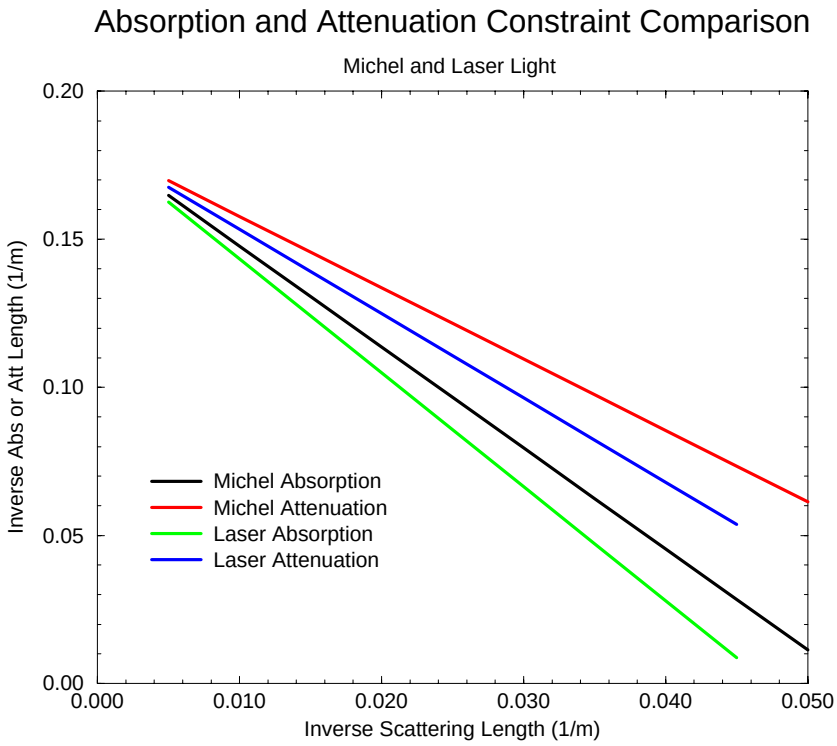

Figure 9: The inverse attenuation length is the sum of the inverse scattering length and the inverse absorption length. Results from the Laser and Michel time distribution measurements are compared. Differences due to wavelength dependence are expected. Measured values of prompt/late light fraction are assumed.

$$\frac{1}{L_A} = \frac{1}{< s >} - \frac{1}{L_S} \frac{1 + \frac{P_{rompt}}{L_{ate}}}{1 - \frac{P_{rompt}}{L_{ate}} \frac{S_{c0}}{C_{h0}}} \tag{15}$$

The result from the Michel analysis is that prompt/late = 2. The mean path for Cherenkov light is not guaranteed to be the same 5.5 m but will not be very different. For the scintillation light the average should be even closer to 5.5 m. Figure 8 shows the constraint relation between scattering length and absorption length for this light source. We see that the attenuation is greater for Cherenkov light. In Figure 9 we make the

direct comparison. We note that the structure of the constraint equations are identical. If one assumes the reported results for prompt/late light, one may solve to find a scintillation fraction which would make the curves the same.

$$\frac{S_{c0}}{C_{h0}} = [1 - \frac{1 + (\frac{P_{rompt}}{L_{ate}})_{Ch}}{1 + (\frac{P_{rompt}}{L_{ate}})_{L}}]/[(\frac{P_{rompt}}{L_{ate}})_{Ch}] \tag{16}$$

We find that $\frac{S_{c0}}{C_{h0}}$=0.11 is the result for the light fractions reported. This should be regarded with suspicion as a determination of the scintillation fraction, however, since we might expect the scattering and absorption to be different for the wavelengths of the Cherenkov and Laser light.

5 Directions for Future Efforts

5.1 Analytic Efforts

In addition the results discussed above, there have been reports on laser light detected from illumination of the MiniBooNE detector with a bare fiber. This data also provides clear evidence of the delayed light response due to scattering in the oil. The geometry is much simpler than that for the Cherenkov light. An analytic analysis of scattering from a single ray [later expanding to the cone angle observed from the bare fiber], should provide a clear comparison with the measured results which would allow one to build confidence in the analytic technique for providing a fitting function. The required steps are a subset of those required for the Cherenkov scattering analysis. This is proposed as the next step in this analysis direction.

One then can explore the scattering for Cherenkov light. Formulas with various considerations included can proceed with various considerations included

1. isotropic scattering
2. scattering of polarized Cherenkov light
3. integration over a Cherenkov spectrum with variable scattering amplitude
4. if initial formulas assumed x =0, consider finite x.

The integrated sensitivity function for scintillation light requires integration over the isotropic emission angles for the scintillation light. One can explore whether this amplitude is sufficient to modify the fitting functions in an interesting way. Probably it is too small to matter.

5.2 Comparisons with Data

Once the analytic forms are available, one can integrate them for comparison with various data sets (laser, Michels, Muons) to confirm the applicability prior to efforts to include the forms into the fitting. The magnitude of scattered light [late light] as a function of the light production point should provide a clear signal. The angular distribution and its time correlation should also be studied.

6 Issues

If scattering must be included in MiniBooNE event fitting, one will need to provide results which we currently do not have. Some issues to be resolved include:

1. The scattering amplitude and the angular, frequency and polarization dependence of the scattering needs to be understood and documented. If we can confirm that it is adequately described by well understood physics, we can use known formulas and verify details for confirmation.

2. We must assume that there is sufficient frequency dependence of the scattering that we will need to know the spectra of the produced light. We should have sufficient knowledge of the oil transmission to provide an effective Cherenkov spectrum from first principles. We need to determine the spectrum of the scintillation. Can we produce sufficient light at IUCF to allow dc measurements with a monochromator?

3. The laser events from both flasks and bare fiber provide strong constraints on the scattering function. Measurements with various laser wavelengths would be very helpful. We have at least three lasers with more under consideration. We could use them to help obtain confidence that we understand the scattering function. Once we have discovered the functional form of the scattering, we can consider whether we can further optimize our tools: more frequencies? polarization?

4. If the scattering amplitude is not too large, one would be able to integrate the scattering assuming a constant light amplitude along the path. If this is not the case, the integration may be more difficult.

7 Conclusions

The time distribution of light from laser pulses and from Michel electrons in the MiniBooNE detector indicate that light scattering provides an important source of late light. Since the source of Cherenkov light is well determined in the fitting procedures, we expect that the scattering amplitude and time distribution can be accurately related to the Cherenkov production. The time delays can be large. The geometry of the Cherenkov cone causes the amplitude of scattered light to vary by large amounts over the surface of the detector. We proposed constructing a scattering amplitude function which will relate the scattering amplitude to the detected time as a function of the Cherenkov emission location and direction.

We have examined relations between scattering, absorption and total attenuation for laser and Michel electron light. The integral of observed time spectra provide relations which relate these quantities and provide bounds on the allowed light transmission model. As we learn more of the physics of the scattering, we may find that additional laser measurements with different emission spectra may be helpful in constraining the optical model of the oil.

We propose constructing the scattering amplitude function analytically, using Mathematica or a similar tool. The function is surely calculable. We expect that we may be able to do the required integrals analytically. If so, we might be fortunate enough to have resulting formulas which can be employed to provide fitting functions to use in fitting the time-amplitude relations for the light.